THE JOURNAL OF PHYSICAL CHEMISTRY B

Article

pubs.acs.org/JPCB

Ultrafast Pump–Probe Study of the Excited-State Charge-Transfer Dynamics in Blue Copper Rusticyanin

Anna Rita Bizzarri,[†] Daniele Brida,[‡] Simona Santini,[†] Giulio Cerullo,[‡] and Salvatore Cannistraro*,[†]

[†]Biophysics and Nanoscience Centre, CNISM, Dipartimento DEB, Università della Tuscia, Viterbo, Italy

[‡]IFN-CNR, Dipartimento di Fisica, Politecnico di Milano, P.za L. da Vinci 32, 20133 Milano, Italy

ABSTRACT: We have used femtosecond pump–probe spectroscopy to investigate the excited-state dynamics of the anticancer blue copper protein rusticyanin, by exciting its ligand to metal charge-transfer band with 25 fs pump pulses centered at 585 nm. The charge-transfer excited state decays exponentially to the ground state with a time constant of about 230 fs, and its recovery is modulated by coherent oscillations. The Fourier transform of the oscillatory component of the signal provides most of the vibrational modes obtained by means of conventional resonance Raman studies, in addition to the low frequency modes below 80 cm^{-1} believed to reflect collective motions of biological relevance.

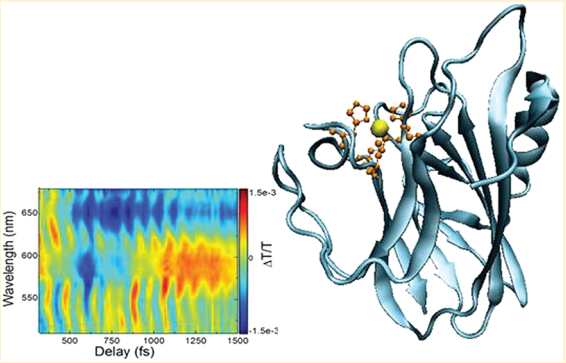

INTRODUCTION

Rusticyanin (Ru) is a 16.6 kDa monomeric type I copper protein involved in the shuttling of electrons within the respiratory transport chain of the acidophilic *Thiobacillus Ferroxidans* bacterium. The core of the molecule consists of a β-sandwich made up of six- and seven-stranded beta-sheets, and analogously to other blue copper proteins, its single copper atom is coordinated with three strong planar ligands His85, Cys138, and His143 and a relatively weaker ligand Met148 in an axial position, with a resulting distorted tetrahedral geometry (Figure 1).[1−4]

In the oxidized form, Ru shows a ligand-to-metal charge transfer (LMCT) absorption band peaking at about 600 nm and arising from a charge-transfer transition from S-Cys to cupric ion,[5] and a very small hyperfine coupling in the parallel region of the electron paramagnetic resonance spectrum.[6] A weaker LMCT band at 450 nm (believed to be associated to a separate Cys-copper charge-transfer transition[7]) and a weak absorption in the near-infrared region (750 nm) can also be observed.

Despite its structural similarity to other blue copper proteins, Ru shows an unusually high redox potential (680 mV),[5,8] which is roughly twice that of any other type I copper protein, and an extreme acid (pH range 1−3) stability.[5,9] These functional peculiarities have been ascribed to the more ordered secondary structure displayed by Ru with respect to other blue copper proteins, deriving from the higher intersheet connectivity, more extensive internal hydrogen bond network, and stronger hydrophobic interactions surrounding the copper active site.[2,10]

Very recently and quite interestingly, it has been shown that Ru shares with another copper protein, azurin, the ability to penetrate human cancer cells and induce either inhibition of the cell cycle progression or apoptosis.[11] It is believed that the azurin anticancer activity stems from its interaction with the tumor suppressor p53 which would result to be stabilized against its Mdm2-mediated proteasomal degradation and can thus activate the apoptotic pathway.[11−14] At variance with azurin, the Ru apoptotic action seems to be only partially mediated by p53 but crucially related to the generation of oxygen reactive species (ROS). This process, that seems

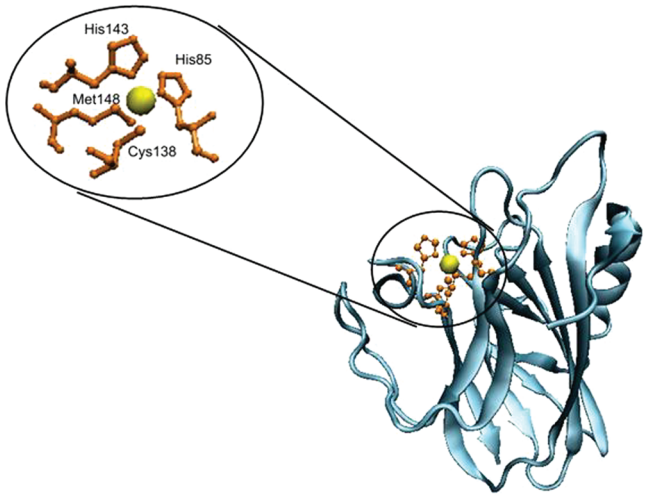

Figure 1. Three-dimensional structure of Ru (PDB entry 1RCY). The copper ion in the northern part of the molecule is represented as a sphere, while the residues coordinating it are represented as balls and sticks. On the left, a schematic picture of the Ru active site is shown.

Received: February 14, 2012
Revised: March 19, 2012
Published: March 20, 2012

dx.doi.org/10.1021/jp301484g | *J. Phys. Chem. B* 2012, 116, 4192–4198

reasonably connected with the Ru electron transfer (ET) properties, could be a peculiarity of all blue copper proteins, including azurin.[15−17]

In this context, it is known that the ET activity and physiological properties of the blue copper proteins are connected with their optical and vibrational features[18] and it is believed that the excitation of these proteins in their LMCT band could mimic the physiological ET process.[19,20] This phenomenon is coupled with the vibrational richness of the active site, as witnessed by the Raman features obtained under resonance conditions with this transition.[21−24] At variance with other blue copper proteins, the spectroscopic properties of Ru are, however, almost unknown. In this paper, we use femtosecond pump−probe spectroscopy to get insight into both the dynamics of the Ru LMCT transition and the Raman modes of the active site. The technique enables the real-time analysis of both the excited state population dynamics and vibrational modes coupled with electronic transitions, even circumventing the experimental difficulties of traditional resonant Raman (RR) in discriminating low-frequency vibrational modes against the laser line.[25] In our resonant pump−probe experiments, the protein is excited in the LMCT band by a pump pulse (whose duration is shorter than the period of the vibrations coupled to the transition) that creates a population in the excited electronic state and vibrational coherences in both the ground and excited states. A delayed probe pulse then interrogates the sample, and its pump-induced transmission change (differential transmission, $\Delta T/T$) is measured by the detector.

Following Ru excitation with 25 fs pulses resonant with the LMCT transition and probing with a broadband visible pulse covering the whole ground state absorption band of Ru, we observed that the charge-transfer excited state decays to the ground state in a single relaxation step with a time constant of about 230 fs. Fourier transform (FT) analysis of the oscillatory pattern superimposed on the signal reveals well-resolved vibrational frequencies almost all coincident with those obtained by means of conventional RR studies, in addition to low-frequency modes below 80 cm^{-1}, which reflect the existence of collective modes, likely having some biological relevance.

EXPERIMENTAL METHODS

Expression and purification of Ru has been performed as reported in ref 11.

Absorption measurements were carried out at room temperature using a two-beam UV−vis spectrophotometer (Jasco V-550) in the spectral region 350−700 nm with a 1 nm bandpass. Absorption spectra of Ru were taken immediately before and after the pump−probe measurements to check that no photodegradation has occurred. Figure 2 shows the optical absorption spectrum, in the visible region, of Ru in 50 mM pH 7.5 sodium phosphate buffer solution at a concentration of 40 μM. The main band peaks at about 595 nm and corresponds to the LMCT transition between S (Cys-pπ) and Cu $d_{x^2-y^2}$.[5] The other band centered at 448 nm, having a lower intensity, is tentatively attributed to a S (Cys-pseudo σ) to Cu $d_{x^2-y^2}$ LCMT transition.[7] The weak band peaking at 750 nm is not shown.

The experimental setup used for the femtosecond pump−probe experiment has been described in detail elsewhere.[26] Briefly, 150 fs pulses centered at 780 nm and with 500 μJ energy at 1 kHz repetition rate, generated by a regeneratively amplified mode-locked Ti:sapphire laser, drive two synchronized visible noncollinear optical parametric amplifiers (NOPAs), the outputs of which are compressed to nearly transform-limited duration by sequences of chirped mirrors. The first NOPA, generating the pump pulses, has a bandwidth limited to ≈20 nm by an interference filter (red dashed line in Figure 2), in order to minimize the solvent-induced artifacts, resulting in 25 fs pulsewidth; the second NOPA generates broadband (500−700 nm) sub-10 fs probe pulses (blue dash-dotted line in Figure 2). The pump and probe pulses are superimposed on the sample in a slightly noncollinear geometry, and their delay is controlled by a motorized translation stage. The pump pulse is modulated at 500 Hz by a chopper wheel. After the sample, the probe beam is focused onto the entrance slit of a spectrometer equipped with a linear photodiode array with a fast electronics allowing a full 1 kHz read-out rate.[27] By recording pump-on and pump-off probe spectra, we calculate the $\Delta T/T$ signal as a function of probe wavelength λ and pump−probe delay τ as $\Delta T/T(\lambda,\tau) = (T_{on}(\lambda,\tau) - T_{off}(\lambda,\tau))/T_{off}(\lambda,\tau)$.

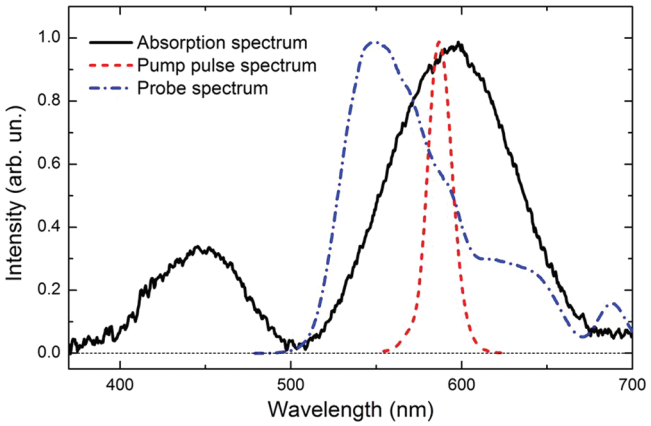

Figure 2. Black solid line: absorption spectrum of Ru (40 μM in phosphate buffer) in the visible region. Red dashed line: spectrum of the pump pulse, centered at 585 nm, with 25 fs duration. Blue dash-dotted line: spectrum of the probe pulse.

The solution (about 10 μL of Ru at a concentration of 2.5 mM in phosphate buffer) was kept in a homemade cuvette employing 200-μm-thick fused silica windows and with an optical path of ≈200 μm.

Raman spectra were recorded in air by a Labram confocal setup (Jobin-Yvon) equipped with a Peltier-cooled CCD detector and a single-grating spectrograph (1800 grooves/mm) allowing a resolution of 5 cm^{-1}. The microscope objective was a 100× with a numerical aperture of 0.9, producing a laser spot size of about 1 μm in diameter. The source was a He−Ne laser (Melles Griot) providing a 632.8 nm radiation with a power emerging from the objective of 6.5 ± 0.5 mW.

RESULTS AND DISCUSSION

Figure 3a shows a two-dimensional plot of $\Delta T/T(\lambda,\tau)$ for Ru following excitation with 25 fs pulses resonant with the transition. Around zero pump−probe delay, at all wavelengths, we observe a strong derivative-like response that lasts for about 50−70 fs. This signal arises from pump−probe cross-phase modulation induced by the nonresonant absorption of the buffer solution, as commonly observed in transient absorption measurements of protein solutions.[20−22] After the buffer response has ceased, a broad $\Delta T/T > 0$ band is present in the region between 550 and 630 nm, at which the strongest

dx.doi.org/10.1021/jp301484g | J. Phys. Chem. B 2012, 116, 4192−4198

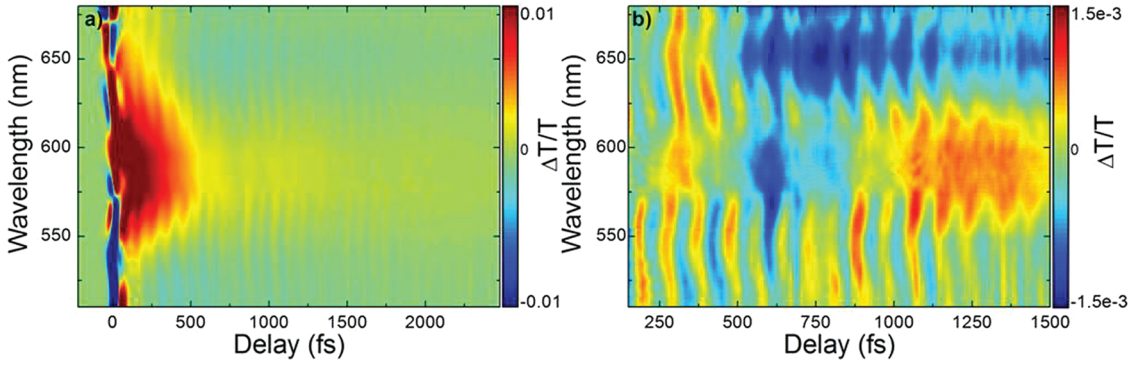

Figure 3. (a) Two-dimensional $\Delta T/T(\lambda,\tau)$ for rusticyanin following excitation by 25 fs pulses at 585 nm. (b) Oscillatory component of the signal, after subtracting the slowly varying component.

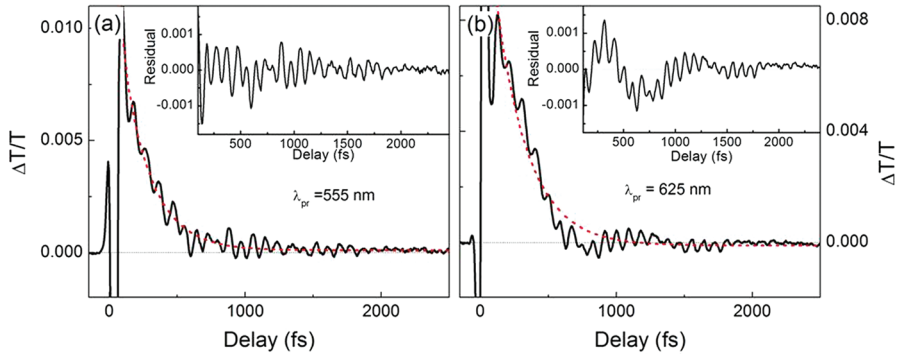

Figure 4. Black solid lines: $\Delta T/T$ dynamics of Ru at two selected probe wavelengths, 555 nm (a) and 625 nm (b); the instantaneous response due to cross-phase modulation in the buffer is not shown to scale. Dashed lines: fits by a single exponential $\Delta T/T(t) = A + Be^{-t/\tau}$; for the 555 nm probe wavelength, we extract τ = 220 fs, $A = 1.9 \times 10^{-5}$, and $B = 1.36 \times 10^{-2}$, while for the 625 nm probe τ = 234 fs, $A = -1.13 \times 10^{-4}$, and $B = 1.43 \times 10^{-2}$. Insets: residuals after subtracting the exponential decay from the $\Delta T/T$ signal.

absorption band of Ru is located (see Figure 2). This band is due to the superposition of photobleaching of the LMCT transition and stimulated emission from the photoexcited state. The signal, which rapidly decays as a consequence of the recovery of the ground-state population, is modulated by a complex oscillatory pattern, that is evident throughout the analyzed time delay and probe wavelength range. This oscillatory activity is better highlighted in Figure 3b, which shows the residuals of the $\Delta T/T$ signal after subtracting the slowly varying background due to population dynamics. The oscillations superimposed on the exponential decay are assigned to the vibrational coherence in the excited and ground electronic states, created by the very short pump pulses.[20]

Figure 4 displays the $\Delta T/T$ dynamics at two selected probe wavelengths (555 and 625 nm) within the absorption band of Ru. Following the instantaneous response due to cross-phase modulation in the buffer, the signal exhibits a rapid decay.

The dynamics has been best-fitted (dashed lines) by an exponential plus a constant offset according to the relationship $\Delta T/T(t) = A + Be^{-t/\tau}$, where A is the constant offset, B is a pre-exponential factor, and τ is the decay time. The fitting parameters are reported in the legend of Figure 4. We note that a small offset constant characterizes the decay trend. As suggested in similar studies,[20−22] this offset could be evidence of a small amount of population becoming trapped on the excited-state surface, preventing the reestablishment of equilibrium on the time-scale of the pump−probe experiment. The extracted decay times are 220 and 234 fs at the probe wavelengths of 555 and 625 nm, respectively; similar values have been extracted for the other probe wavelengths. Generally, these rapid decay times indicate that most of the excited state population created by the pump pulse quickly returns to the ground state (or states) in a nonradiative fashion by an ultrafast internal conversion (IC) process. Since these electronic transitions involve the movement of charge from ligand atoms to the copper center, the decay of excited state population can be likely assigned to a return charge transfer process.[20]

Notably, the decay times of Ru are very close to those measured by pump−probe experiments for other copper proteins. More specifically, Nakashima et al. observed a 270 fs decay time for the ground-state recovery in plastocyanin from *Synechococcus* when excited with a 33 fs pulse at 635 nm.[23] Cimei et al. have investigated azurin and poplar plastocyanin by exciting the sample with a 10 fs pulse centered at 550 nm and analyzing the differential transmission at 580 and 560 nm.[21,22] In both cases, they found a single exponential decay with a time constant of about 270 fs. Book et al. reported pump−probe measurements, for poplar and spinach plastocyanins and human ceruloplasmin, by exciting with 16 fs pulses centered at 770 nm and investigating both the integrated and spectrally resolved (750 and 800 nm spectral components) probe signals, finding an exponential decay of the excited state with a time constant of about 280 fs.[20] Longer decay times (in the range 270−700 fs), even depending on the probe wavelength, have been instead observed for umecyanin from horseradish root upon excitation at 600 nm;[24] such a behavior has been ascribed

dx.doi.org/10.1021/jp301484g | J. Phys. Chem. B 2012, 116, 4192−4198

to a larger energy gap between ligand and metal orbitals in umecyanin, with respect to other copper proteins.

Following the ground state recovery, the $\Delta T/T$ signal changes sign to the red and the blue of the Ru main absorption spectrum, displaying two weak photoinduced absorption (PA) bands, which then decay on the 2 ps time scale. This behavior, already visible in the $\Delta T/T$ map of Figure 3a, is highlighted in Figure 5, showing zooms of the $\Delta T/T$ dynamics at two probe

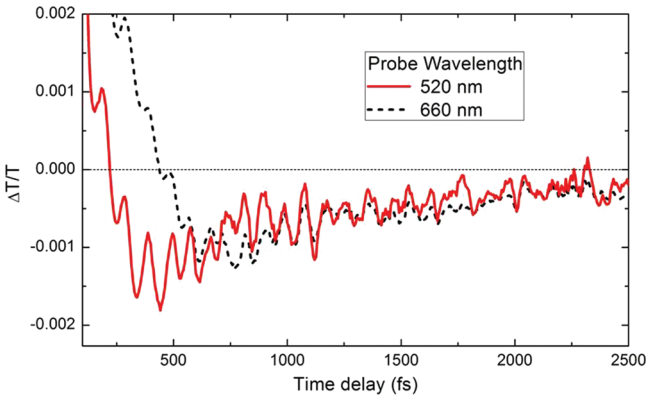

Figure 5. Zooms of the $\Delta T/T$ dynamics at probe wavelengths to the red of the main (660 nm) and the higher energy (520 nm) absorption bands. The observed PA is assigned to hot ground state absorption.

wavelengths in the red (660 nm) and in the blue (520 nm). This PA signal is most likely due to absorption by hot ground state molecules that are formed by the IC process. In a nonradiative electronic transition, the energy of the excited molecule is not emitted in the form of a photon but remains localized on the molecule and its immediate environment. Therefore, the molecule is left in a nonequilibrium ground state, with excess vibrational energy, which results in a red-shift of the ground state absorption spectrum.[28] Hot ground state absorption produces a PA signal at lower probe photon energies with respect to the ground state absorption band. In our case, we observe PA bands to the red of the 595 and 448 nm bands, which decay with a time constant of τ = 760 fs, typical of vibrational relaxation in the ground state.[29]

Notably, the evidence that Ru shares with other blue copper proteins the order of magnitude of the decay time as well as the dynamics of the ground state recovery suggests that all these proteins are characterized by similar organization of their electronic levels within the active site. The fact that Ru has a redox potential much higher than that usually measured for other copper proteins seems to indicate that the levels of the electronic states involved in the pump−probe are not affected by the redox potential. This finds a correspondence with the fact that the redox potential is regulated by a fine-tuning of many different factors, such as the protein matrix composition and spatial organization, the details in the active site structure, etc.[30] On the other hand, it is interesting to remark that all of these proteins share a marked anticancer activity which could be, in some way, related to their active site properties. Certainly, both the hydrophobicity of the active site and the redox activity of blue copper proteins are crucial aspects for their antiproliferative action.[31,32] The former may favor the interaction with the intracellular partners triggering the apoptotic process, while the presence of redox proteins in the cytosol may signal to the cell the occurrence of a failure of the energetic generation and could lead to the initiation of the apoptotic process. In addition, and more interestingly, it has been shown that azurin and Ru anticancer activity is related with the intracellular levels rise of ROS.[11,12] On such a basis, it could be hypothesized that the anticancer activity of Ru could be, in some way, connected with its ET capability.

In order to analyze the oscillatory component of the signal, we have preliminarily subtracted the fitting exponential decay from the experimental data. The residuals, shown in Figure 3b and in the insets of Figure 4, exhibit slow oscillations superimposed on the fast ones around the zero level. These signals have been then analyzed in the frequency domain by FT to extract the frequencies of the single vibrational components. As already mentioned, our approach, known as impulsive coherent vibrational spectroscopy or impulsive stimulated Raman scattering (ISRS),[33] allows determining vibrational coherences in the time domain, well complementing conventional frequency-domain Raman spectroscopy. The FT amplitudes of the oscillatory components of the signal probed at 555 and 625 wavelengths are shown in Figure 6, where some

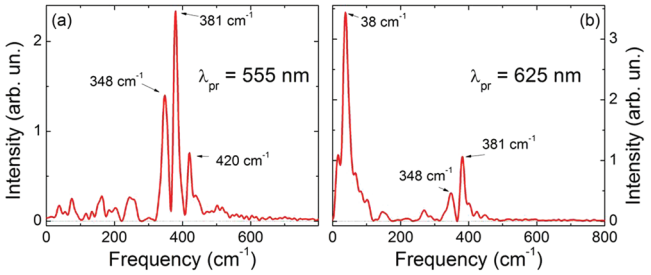

Figure 6. FT power spectra of the oscillatory components of signals shown in the insets of Figure 4.

clear peaks located mainly below 500 cm^{-1} emerge. We remark that, although the relative intensity of the peaks slightly varies in the FT signals detected at other wavelengths, their positions result to be essentially unchanged in all the cases. The most prominent vibrational modes are located in the 350−450 cm^{-1} region. In particular, two intense peaks are detected at 348 and 381 cm^{-1} and a less marked peak at 420 cm^{-1} (see the wavenumbers indicated in Figure 6). A rather strong peak is also observed in the low frequency region (at about 38 cm^{-1}) together with a smaller peak at about 78 cm^{-1}. Other peaks are evident in the region between 150 and 270 cm^{-1}.

The measured coherent oscillation could be assigned to vibrational wavepacket motion on either the ground state or the excited state potential energy surface (PES). Pump−probe spectroscopy involves a three-field interaction with the sample; two of these with the pump, creating a population, and one with the probe, creating a nonlinear polarization which is read by a further interaction with the probe pulse. For short pump pulses, two fields in the pump pulse can excite a vibrational wavepacket oscillating on the excited state PES. Another possibility is that the first field induces a polarization wavepacket on the excited state PES, which then propagates for some time during the pump pulse so that the second pump field brings the wavepacket back down to the ground state, displaced from the equilibrium position. In this way, ground state oscillations are generated by the ISRS mechanism.[34] Assignment of the observed coherence to the ground or to the excited state is critically dependent on a comparison with RR spectra, and on amplitude, phase, and damping times of the observed oscillations. Figure 7a reports the probe wavelength

dx.doi.org/10.1021/jp301484g | J. Phys. Chem. B 2012, 116, 4192−4198

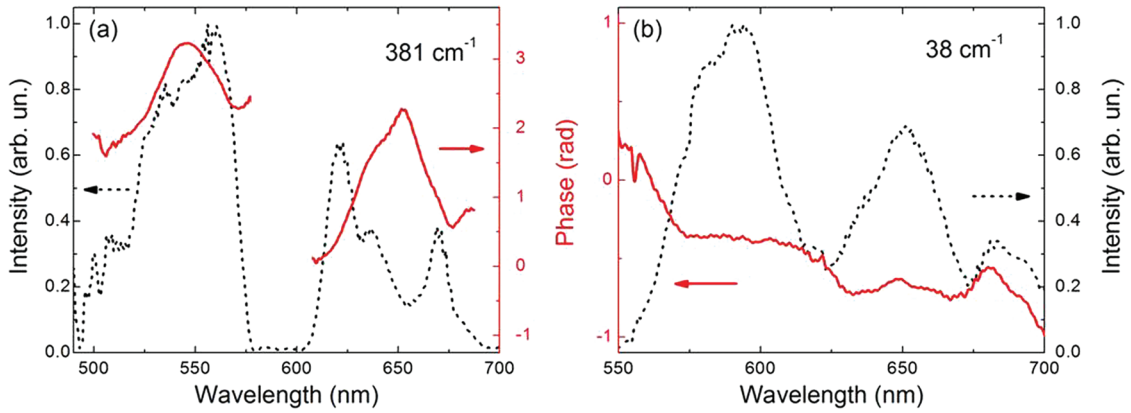

Figure 7. Probe wavelength dependence of amplitude and phase of the oscillations for the most prominent high-frequency (380 cm^{-1}, (a)) and low-frequency (38 cm^{-1}, (b)) modes.

dependence of amplitude and phase of the oscillations for the most prominent high-frequency mode (381 cm^{-1}). The amplitude of the modulation vanishes close to the ground state absorption maximum, while the phase shows a 180° jump around this absorption maximum. Both of these features are consistent with a wavepacket oscillating on the ground state PES,[35] for which a minimum of oscillation amplitude should occur at the absorption peak, while a π phase shift is expected between oscillations to the red and to the blue of the absorption maximum. This assignment is also consistent with the fact that the oscillations present a damping time of ≈1.2 ps (see insets of Figure 4) which is significantly longer than the excited state lifetime. An additional motivation for the assignment to the ground state is the agreement with the RR spectrum (see next paragraph). For the low-frequency mode at 38 cm^{-1}, the probe wavelength dependence of amplitude and phase of the oscillations is reported in Figure 7b: in this case, assignment to the ground state is not straightforward.

The bands in the 350−450 cm^{-1} region are enhanced via excitation of Ru strong 600 nm absorption band, as it is observed in the traditional RR spectrum of blue copper proteins. These bands should then be analyzed in connection with the vibrational features appearing in the RR spectrum of Ru. Since the Raman spectrum of Ru is not known, we have carried out a Raman investigation of Ru by standard Raman spectroscopy. Figure 8 shows the RR spectrum of Ru obtained upon resonant excitation at 632.8 nm, in aqueous solution at the same concentration used in the pump−probe experiments. Even if the Raman signal is rather noisy, some clear peaks can be evidenced from the spectrum. In particular, two intense peaks at 378 and 416 cm^{-1} together with some shoulders around 350 and 430 cm^{-1} can be observed (see the wavenumbers indicated in Figure 8). These modes around 400 cm^{-1}, which constitute in general the fingerprint of the RR spectra of blue copper proteins, can be assigned to the mixing of the Cu−S(Cys) stretching vibration with multiple heavy atom bending modes of the ligand and adjacent residues.[36] Additionally, the band at about 270 cm^{-1} can be attributed to the Cu−N stretch from hystidine ligands of the copper ion.[36,37] Finally, the rather large bands at about 750−850 cm^{-1} are overtones of the resonant bands around 400 cm^{-1}.

From a comparison with the Fourier spectrum in Figure 6, it comes out that almost all the vibrational features observed in the RR spectrum of Ru find a very good correspondence with some of the peaks emerging from the pump−probe experiment.

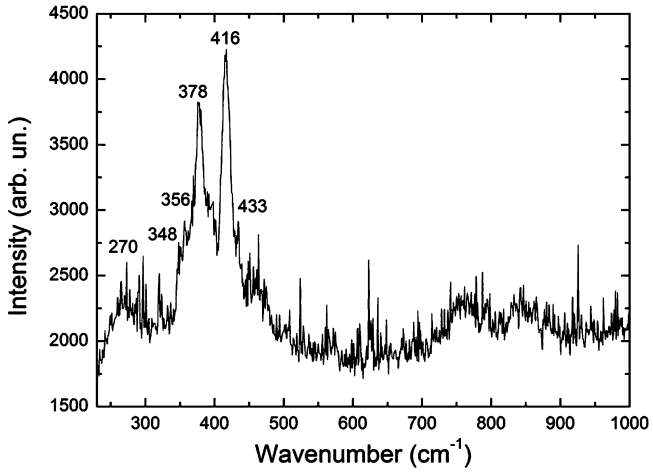

Figure 8. RR spectrum of Ru at a concentration of 2.5 mM obtained by a 632.8 nm laser radiation.

However, the Fourier spectrum has a higher richness in the spectral content with respect to the RR spectroscopy, as also observed in other cases.[21,22,24] Additionally, the slight shift measured in the positions of the pump−probe peaks with respect to that of the conventional RR finds a correspondence with what was detected in other studies.[21,22,36,37] In this respect, we remark that the RR vibrational features of Ru are rather similar to those observed in other blue copper proteins, characterized by similar organization of the copper active site.[38,39] Slight modulations in the positions of the main peaks could be put into a relationship with differences in the copper active site as well as in the surrounding protein matrix.

Now, we would like to discuss the vibrational features detected in the Fourier spectrum in the low frequency region which, on the contrary, cannot be easily investigated by standard Raman spectroscopy. Generally, low-frequency modes at about 20−80 cm^{-1} have been observed in copper, and even other proteins, by the pump−probe and by inelastic neutron scattering.[20−22,40] These modes (especially that at 38 cm^{-1}) deserve particular attention in proteins, since they have been put into a relationship with the existence of delocalized modes, inherent to collective vibrations, with large amplitude and involving the whole protein skeleton.[23,41] The possibility that these modes could be coupled to the optical excitation has also been hypothesized. Notably, these low frequency modes are reminiscent of the so-called boson peak, which is a vibrational

dx.doi.org/10.1021/jp301484g | J. Phys. Chem. B 2012, 116, 4192−4198

fingerprint of amorphous systems.[40] On such a basis, these low frequency modes can be assumed to provide evidence for the amorphous character of protein systems.[42] In this respect, we mention that some of the authors have also put into evidence the existence of similar modes in the hydration water around plastocyanin, by suggesting a strong dynamical coupling between the protein and the surrounding hydration water.[43] On the other hand, it has been speculated about the possibility that these low frequency modes might deserve some biological relevance; e.g., they could be involved in the biorecognition process within biological partners.[44]

CONCLUSIONS

In this paper, we carried out femtosecond pump−probe experiments on the copper protein Ru in aqueous solution. Electronic relaxation and coherent vibrational dynamics have been simultaneously measured by real-time vibrational spectroscopy. Upon excitation with 25 fs pulses resonant with the LMCT transition, we observed ground state recovery with a time constant of about 230 fs, indicative of a strong nonradiative coupling between the ground and excited electronic states. This decay time is notably very close to that measured for the other blue copper proteins, suggesting that Ru functional peculiarities cannot be ascribed to particular features of the electronic state organization. On the other hand, the coherence created by the short pulses in the ground and excited state allowed us to reveal vibrational features of both of these states. In particular, we found vibrational modes in the 350−450 cm^1 region, also detectable with RR and which are typical of most blue copper ET proteins. Additionally, we have registered some low frequency bands, in the 20−80 cm^{-1} region, which are connected with protein collective modes, probably reflecting some functional features. With both the decay time and vibrational features of Ru being very similar to those of other blue copper proteins, the peculiar functional and structural features seem to not be connected to the LMCT dynamics and then to the ET properties.

It has recently been demonstrated that Ru shares with other blue copper proteins an anticancer activity, strictly connected with ROS generation. Since the Ru ET properties are similar to those of other type I copper proteins, it would be interesting to investigate whether the generation of oxygen radical species is due to the Ru ET properties or to its high redox potential.

AUTHOR INFORMATION

Corresponding Author

*E-mail: cannistr@unitus.it. Phone/Fax: 0761/357136.

Notes

The authors declare no competing financial interest.

ACKNOWLEDGMENTS

This work was partly supported by a grant from the Italian Association for Cancer Research (AIRC, IG 10412) and by a PRIN-MIUR 2009 project (no. 2009WPZM4S). We would like to warmly thank Prof. Craig W. Beattie (Department of Surgical Oncology, University of Illinois College of Medicine, Chicago) for providing us the Ru.

REFERENCES

(1) Ronk, M.; Shively, J. E.; Shute, E. A.; Blake, R. C. II. *Biochemistry* **1991**, *30*, 9435−9442.
(2) Walter, R. L.; Ealick, S. E.; Friedman, A. M.; Blake, R. C. II; Proctor, P.; Shoham, M. *J. Mol. Biol.* **1996**, *263*, 730−751.
(3) Cobley, J. G.; Haddock, B. A. *FEBS Lett.* **1975**, *60*, 29−33.
(4) Yamanaka, T.; Fukumori, Y. *FEMS Microbiol. Rev.* **1995**, *17*, 401−13.
(5) Cox, J. C.; Boxer, D. H. *Biochem. J.* **1978**, *174*, 497−502.
(6) Cox, J. C.; Aasa, R.; Malmström, B. G. *FEBS Lett.* **1978**, *93*, 157−160.
(7) Hall, J. F.; Kanbi, L. D.; Harvey, I.; Murphy, L. M.; Hasnain, S. S. *Biochemistry* **1998**, *37*, 11451−11458.
(8) Ingledew, W. J.; Cobley, J. G. *Biochim. Biophys. Acta* **1982**, *590*, 141−158.
(9) Blake, R. C. II; Shute, E. A. *J. Biol. Chem.* **1987**, *262*, 14983−14989.
(10) Botuyan, M. V.; Toy-Palmer, A.; Chung, J.; Blake, R. C. II; Beroza, P.; Case, D. A.; Dyson, H. J. *J. Mol. Biol.* **1996**, *263*, 752−767.
(11) Yamada, T.; Hiraoka, Y.; Das Gupta, T. K.; Chakrabarty, A. M. *Cell Cycle* **2004**, *3*, 1182−1187.
(12) Yamada, T.; Goto, M.; Punj, V.; Zaborina, O.; Chen, M. L.; Kimbara, K.; Majumdar, D.; Cunningham, E.; Das Gupta, T. K.; Chakrabarty, A. M. *Proc. Natl. Acad. Sci. U.S.A.* **2002**, *99*, 14098−14103.
(13) Taranta, M.; Bizzarri, A. R.; Cannistraro, S. *J. Mol. Recognit.* **2008**, *21*, 63−70.
(14) Domenici, F.; Fiasconi, M.; Mazzei, F.; D'Orazi, G.; Bizzarri, A. R.; Cannistraro, S. *J. Mol. Recognit.* **2011**, *24*, 707−714.
(15) Yamada, T.; Hiraoka, Y.; Ikehata, M.; Kimbara, K.; Avner, B. S.; Das Gupta, T. K.; Chakrabarty, A. M. *Proc. Natl. Acad. Sci. U.S.A.* **2004**, *101*, 4770−4775.
(16) Liu, B.; Chen, Y.; St. Clair, D. K. *Free Radical Biol. Med.* **2008**, *44*, 1529−1535.
(17) Méplan, C.; Richard, M.-J.; Hainaut, P. *Biochem. Pharmacol.* **2000**, *59*, 25−33.
(18) Delfino, I.; Cannistraro, S. *Biophys. Chem.* **2009**, *139*, 1−7.
(19) Edington, M. D.; Diffey, W. M.; Doria, W. J.; Riter, R. E.; Beck, W. F. *Chem. Phys. Lett.* **1997**, *275*, 119−126.
(20) Book, L. D.; Arnett, D. C.; Hu, H.; Scherer, N. F. *J. Phys. Chem. A* **1998**, *102*, 4350−4359.
(21) Cimei, T.; Bizzarri, A. R.; Cannistraro, S.; Cerullo, G.; De Silvestri, S. *Chem. Phys. Lett.* **2002**, *362*, 497−503.
(22) Cimei, T.; Bizzarri, A. R.; Cerullo, G.; De Silvestri, S; Cannistraro, S. *Biophys. Chem.* **2003**, *106*, 221−231.
(23) Nakashima, S.; Nagasawa, Y.; Seike, K.; Okada, T.; Sato, M.; Kohzuma, T. *Chem. Phys. Lett.* **2000**, *331*, 396−402.
(24) Delfino, I.; Manzoni, C.; Sato, K.; Dennison, C.; Cerullo, G.; Cannistraro, S. *J. Phys. Chem. B* **2006**, *110*, 17252−17259.
(25) Johnson, A. E.; Myers, A. B. *J. Chem. Phys.* **1996**, *104*, 2497−2507.
(26) Manzoni, C.; Polli, D.; Cerullo, G. *Rev. Sci. Instrum.* **2006**, *77*, 023103/1−023103/9.
(27) Polli, D.; Lüer, L.; Cerullo, G. *Rev. Sci. Instrum.* **2007**, *78*, 103108−103117.
(28) Pecourt, J.-M. L.; Peon, J.; Kohler, B. *J. Am. Chem. Soc.* **2001**, *123*, 10370−10378.
(29) Lenz, K.; Pfeiffer, M.; Lau, A.; Elsaesser, T. *Chem. Phys. Lett.* **1994**, *229*, 340−346.
(30) Van den Bosch, M.; Swart, M.; Snijders, J. G.; Berendsen, H. J.; Mark, A. E.; Oostenbrink, C.; Van Gunsteren, W. F.; Canters, G. W. *ChemBioChem* **2005**, *6*, 738−746.
(31) Punj, V.; Chakrabarty, A. M. *Cell. Microbiol.* **2003**, *5*, 225−231.
(32) Yamada, T.; Hiraoka, Y.; Das Gupta, T. K.; Chakrabarty, A. M. *Cell Cycle* **2004**, *3*, 752−755.
(33) Kahan, A.; Nahmias, O.; Friedman, N.; Sheves, M.; Ruhman, S. *J. Am. Chem. Soc.* **2007**, *129*, 537−546.
(34) Ruhman, S.; Kohler, B.; Joly, A. G.; Nelson, K. A. *Chem. Phys. Lett.* **1987**, *141*, 16−24.
(35) Kumar, A. T. N.; Rosca, F.; Widom, A.; Champion, P. M. *J. Chem. Phys.* **2001**, *114*, 701−724.

(36) Loppnow, G. R.; Fraga, E. *J. Am. Chem. Soc.* **1997**, *119*, 896−905.
(37) Qiu, D.; Dong, S.; Ybe, J. A.; Hecht, M. H.; Spiro, T. G. *J. Am. Chem. Soc.* **1995**, *117*, 6443−6446.
(38) Thamann, T. J.; Franko, P.; Willis, L. J.; Loehr, T. M. *Proc. Natl. Acad. Sci. U.S.A.* **1982**, *79*, 6396−6400.
(39) Han, J.; Adman, E. T.; Beppu, T.; Codd, R.; Freeman, H. C.; Huq, L.; Loehr, T. M; Sanders-Loehr, J. *Biochemistry* **1991**, *30*, 10904−10913.
(40) Paciaroni, A.; Stroppolo, M. E.; Arcangeli, C.; Bizzarri, A. R.; Desideri, A.; Cannistraro, S. *Eur. Biophys. J.* **1999**, *28*, 447−456.
(41) Nagasawa, Y.; Fujita, K.; Katayama, T.; Ishibashi, Y.; Miyasaka, H.; Takabe, T.; Nagao, S.; Hirota, S. *Phys. Chem. Chem. Phys.* **2010**, *12*, 6067−6075.
(42) Bizzarri, A. R.; Paciaroni, A.; Cannistraro, S. *Phys. Rev. E* **2000**, *62*, 3991−3999.
(43) Paciaroni, A.; Bizzarri, A. R.; Cannistraro, S. *Phys. Rev. E* **1999**, *60*, 2476−2479.
(44) Zhou, H. X.; Wlodek, S. T.; McCammon, J. A. *Proc. Natl. Acad. Sci. U.S.A.* **1998**, *95*, 9280−9283.